Report

Cell Reports

Whisking-Related Changes in Neuronal Firing and Membrane Potential Dynamics in the Somatosensory Thalamus of Awake Mice

Graphical Abstract

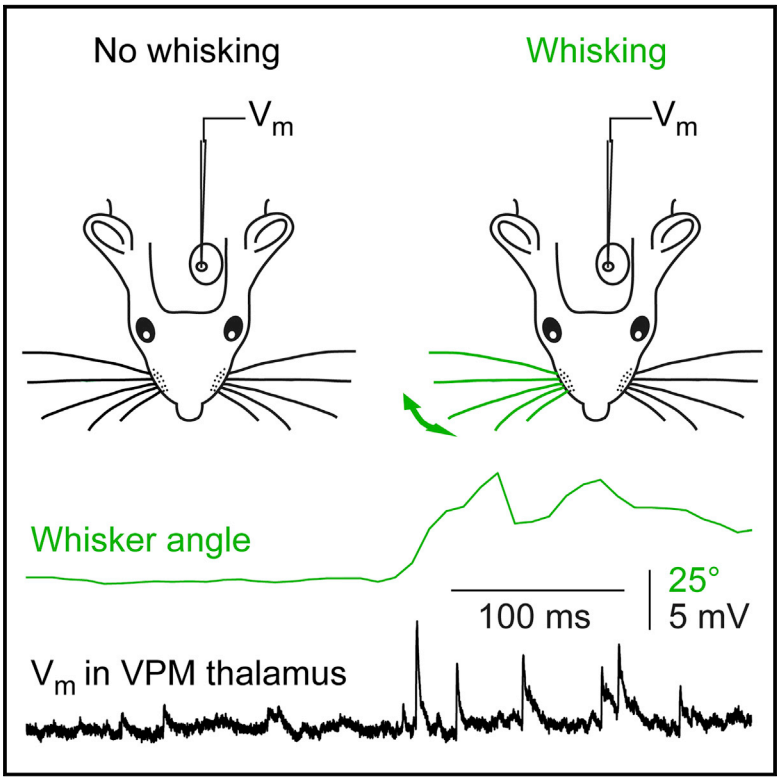

Authors

Nadia Urbain, Paul A. Salin, Paul-Antoine Libourel, Jean-Christophe Comte, Luc J. Gentet, Carl C.H. Petersen

Correspondence

nadia.urbain@inserm.fr

In Brief

Urbain et al. measure membrane potential and action potential firing in the somatosensory thalamus of awake mice during whisker movement. Whisking increased large fast synaptic inputs specifically in VPM cells. Compared to Pom neurons, VPM cells increased firing more strongly during whisking and were more strongly modulated by whisking phase.

Highlights

- Intracellular and extracellular recordings in somatosensory thalamus of awake mice
- State dependence and heterogeneity of activity of thalamic cells
- During whisking, selective increase in fast-rising EPSPs in VPM neurons
- Whisking-cycle phase-locked action potential firing in a subset of VPM neurons

Urbain et al., 2015, Cell Reports *13*, 647–656
October 27, 2015
http://dx.doi.org/10.1016/j.celrep.2015.09.029

CellPress

Cell Reports
Report

Whisking-Related Changes in Neuronal Firing and Membrane Potential Dynamics in the Somatosensory Thalamus of Awake Mice

Nadia Urbain,[1,2,*] Paul A. Salin,[2] Paul-Antoine Libourel,[2] Jean-Christophe Comte,[3] Luc J. Gentet,[3] and Carl C.H. Petersen[1]
[1]Laboratory of Sensory Processing, Brain Mind Institute, Faculty of Life Sciences, Ecole Polytechnique Fédérale de Lausanne (EPFL), Lausanne 1015, Switzerland
[2]Physiopathologie des Réseaux Neuronaux du Cycle Sommeil, Centre de Recherche en Neurosciences de Lyon, INSERM U1028-CNRS UMR5292, Université Claude-Bernard-Lyon 1, 69372 Lyon, France
[3]Integrated Physiology of Brain Arousal Systems, Centre de Recherche en Neurosciences de Lyon, INSERM U1028-CNRS UMR5292, Université Claude-Bernard-Lyon 1, 69372 Lyon, France
*Correspondence: nadia.urbain@inserm.fr
http://dx.doi.org/10.1016/j.celrep.2015.09.029

SUMMARY

The thalamus transmits sensory information to the neocortex and receives neocortical, subcortical, and neuromodulatory inputs. Despite its obvious importance, surprisingly little is known about thalamic function in awake animals. Here, using intracellular and extracellular recordings in awake head-restrained mice, we investigate membrane potential dynamics and action potential firing in the two major thalamic nuclei related to whisker sensation, the ventral posterior medial nucleus (VPM) and the posterior medial group (Pom), which receive distinct inputs from brainstem and neocortex. We find heterogeneous state-dependent dynamics in both nuclei, with an overall increase in action potential firing during active states. Whisking increased putative lemniscal and corticothalamic excitatory inputs onto VPM and Pom neurons, respectively. A subpopulation of VPM cells fired spikes phase-locked to the whisking cycle during free whisking, and these cells may therefore signal whisker position. Our results suggest differential processing of whisking comparing thalamic nuclei at both sub- and supra-threshold levels.

INTRODUCTION

Most of our sensory experiences are gained by active exploration of the world, requiring movements of sensory organs. Rodents rhythmically move their whiskers forward and backward to explore and discriminate objects in their immediate environment. Active vibrissal sensation is mediated by a hierarchical array of parallel and nested motor-sensory loops (Kleinfeld et al., 2006; Kleinfeld and Deschênes, 2011). Sensory vibrissal information is relayed to the neocortex by trigemino-thalamic pathways, where the thalamus is the main gateway of vibrissal transmission to the cerebral cortex (for review, see Bosman et al., 2011). The thalamus is composed of several nuclei, two of which are thought to be critically involved in the transmission of whisker sensation to the somatosensory barrel cortex (S1). These are the ventral posterior medial nucleus (VPM) and the posterior medial group (Pom), which receive distinct vibrissal inputs from two nuclei of the brainstem trigeminal complex, respectively, the principalis (PrV) and the interpolaris (SpVi).

It has been suggested that whisker-object contact and whisker position during free whisker movement might be encoded by different parallel pathways (Yu et al., 2006, 2015). Convergent studies are consistent with the hypothesis that the lemniscal pathway, through the VPM, is required for high-resolution encoding of contact information, necessary for texture and shape discrimination (for review, see Deschênes et al., 2005). However, the role of the paralemniscal pathway through the Pom in the encoding of whisker position and movement remains controversial (Yu et al., 2006, 2015; Masri et al., 2008; Ahissar et al., 2008). Our current knowledge of thalamic processing in the whisker sensorimotor system is based largely on recordings from anesthetized rats; but, to uncover the functional relevance of these parallel sensory pathways, measurements in awake animals during whisker-related behavior are required. Here we combined extracellular or intracellular recordings of thalamic projection neurons in VPM and Pom together with high-speed filming of whisker movements and recordings of cortical and behavioral states in order to advance the understanding of active sensing in the thalamus of awake mice.

RESULTS

We performed extracellular and intracellular recordings of thalamic relay cells while simultaneously measuring the electroencephalogram (EEG), S1 local field potential (LFP), and electromyogram (EMG) of neck muscles together with high-speed video-tracking of whisker movements in head-restrained mice (Figure 1A). These measurements allowed us to analyze thalamic activity and membrane potential (V_m) or action potential (AP) firing in relationship to different cortical and behavioral states

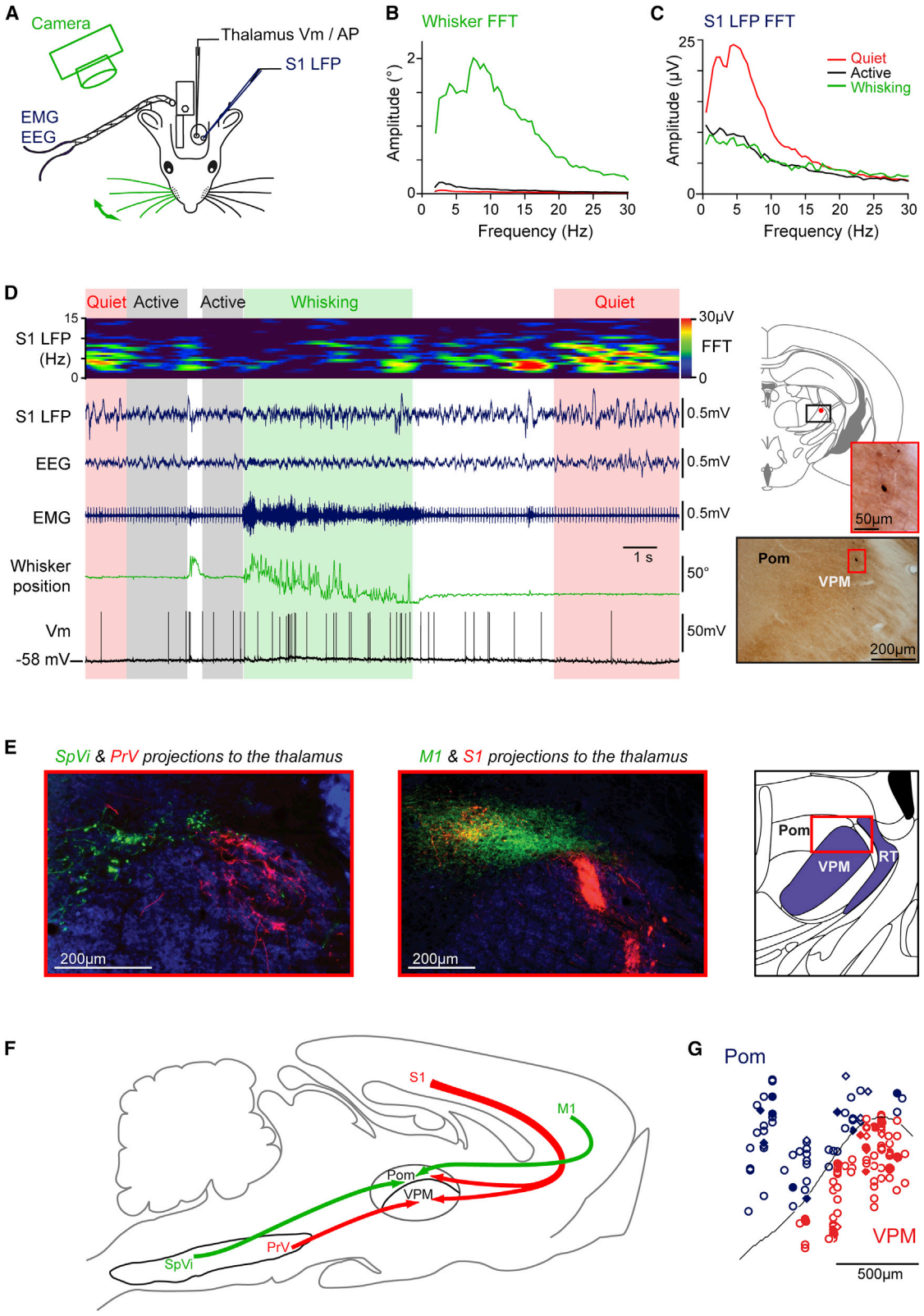

Figure 1. Recording Thalamic Activity in Awake Head-Restrained Mice during Quantified Whisker Behavior

(A) Schematic of experimental setup. Extracellular or intracellular thalamic recordings were performed in awake head-restrained mice together with measurement of cortical LFP, EEG, and EMG. Whisker movements were filmed with a high-speed camera.

(legend continued on next page)

(Figure 1). In this paper, we focus on thalamic activity during waking states.

Distinct States of Wakefulness

Quiet wakefulness (quiet) was characterized by large-amplitude slow LFP and EEG fluctuations and the absence of whisker movements (for review, see Zagha and McCormick, 2014; Figures 1B–1D and S1A). Active cortical states were characterized by small-amplitude fast LFP and EEG fluctuations, without whisking (active) or with whisking (whisking). Low-frequency spectral power (0.5–5 Hz) during quiet states was significantly larger than during active or whisking states, while high-frequency spectral power (30–80 Hz) during whisking was significantly larger than during quiet or active states (averaged across 68 cells recorded from 24 mice; $p < 0.001$ in both cases, ANOVA for repeated measures).

Recordings in the Somatosensory Thalamus

We recorded thalamic neurons across distinct vigilance states (Figure 1D). Last recorded cells were labeled with Neurobiotin (extracellular, n = 11 of 121 cells; intracellular, n = 9 of 21 cells; n = 24 mice), allowing their precise location to be determined in relationship to the boundary between VPM and Pom.

The VPM is densely innervated by PrV and S1, whereas the Pom is strongly innervated by SpVi, S1, and motor cortex (M1) (n = 2 mice for trigeminal tracer injections and n = 3 mice for cortical tracer injections) (Figures 1E, 1F, and S1C). The location of the recorded neurons within the somatosensory thalamus is, therefore, likely to be important, and, accordingly, we separately analyzed neurons in VPM and Pom (Figure 1G; see the Supplemental Experimental Procedures). Cells located in the Pom/VPM transition zone (see the Supplemental Experimental Procedures) behaved as an intermediate and highly heterogeneous group, in agreement with a previous study (Slézia et al., 2011), and these cells in the transition zone were not included in our analyses.

Thalamic Extracellular Firing as a Function of Cortical State and Behavior

Thalamic AP firing was tightly correlated with cortical and behavioral states (Figures 2A, 2B, and S2; Fanselow and Nicolelis, 1999; Poulet et al., 2012). We found close correlations between VPM and Pom cell AP firing rate and EEG, LFP, and EMG envelopes during wakefulness (Figure S1B). Thalamic firing rates increased significantly when the mouse switched from the quiet to the active state (VPM: quiet 3.8 ± 0.4 Hz, active 10.9 ± 0.8 Hz, n = 56 cells; Pom: quiet 3.8 ± 0.3 Hz, active 9.4 ± 0.7 Hz, n = 33 cells; Figure 2C; Table S1). During quiet and active states, there were no differences in firing rates comparing VPM and Pom neurons. In contrast, during whisking we observed a further increase in firing rate, beyond that of the active state, selectively in VPM (15.3 ± 1.0 Hz, n = 56 cells) compared with Pom (11.3 ± 0.9 Hz, n = 33 cells). It is important to note that we observed heterogeneity across recordings in both VPM and Pom (Figure 2D), with 61% of neurons in VPM and 42% of neurons in Pom increasing firing rate by more than 20% during whisking compared to active states, whereas 9% of VPM neurons and 24% of Pom neurons decreased firing rate by more than 20%.

Analysis of burst firing (bouts of high-frequency spike trains) showed that the activity of the VPM cells is significantly altered between whisking and active states, in contrast to the activity of Pom cells. For this quantification, we defined a burst as a sequence of APs starting when two spikes occurred within 10 ms, ending when interspike interval (ISI) was more than 15 ms. VPM cells exhibited significantly more bursts during whisking compared to the active or quiet state (Figures 2E, 2F, and S2B; Table S1; VPM, n = 49 cells; Pom, n = 29 cells), switching back to a tonic activity between whisking episodes. Such a modification of the firing pattern was not observed in Pom cells. The ISI histograms calculated for VPM cells during whisking were best fitted with two log-normal distributions (Figure 2G; n = 28 cells; see the Supplemental Experimental Procedures), one for the 1- to 10-ms interval and the other for the 11- to 200-ms interval. In contrast, the ISI histograms computed for Pom cells can be fitted by a single log-normal distribution (Figure 2G; n = 9 cells), corresponding to the fitting curve of the 11- to 200-ms ISIs of VPM cells. The fraction of 1- to 10-ms ISIs increased significantly in the whisking state compared with the active state specifically for VPM cells (Figure S2C). This was not observed in Pom cells. Furthermore, the mean duration of 1- to 10-ms ISIs was significantly shorter for VPM cells compared with Pom cells, while no difference was observed between the two nuclei in the mean duration of 11- to 200-ms ISIs (Figure S2D).

In addition, the temporal relationship between thalamic firing and cortical activity was analyzed by computing averages of the S1-LFP triggered on thalamic spikes across waking states (Figure S2E). The population spike-triggered average (STA) calculated for both VPM and Pom cells revealed correlated

(B) Grand average Fast Fourier Transform (FFT) of whisker position across quiet, active, and whisking states (averaged across 68 cells recorded from 24 mice) is shown.

(C) Grand average FFT of S1-LFP across quiet, active, and whisking states (averaged across 68 cells recorded from 24 mice) is shown.

(D) Example experiment across quiet, active, and whisking states with (from top to bottom) sliding window FFT (color graph) of the S1-LFP (blue), EEG (blue), neck EMG (blue), whisker position (green), and V_m (black) of a cell in the VPM. Mean V_m for this cell was as follows: quiet −58.5 mV, active −56.1 mV, whisking −54.9 mV. Coronal brain sections counterstained with cytochrome oxidase (right) show the location of the recorded neuron in the VPM.

(E) Coronal section showing the anterograde labeling in the thalamus after BDA (red) and PHA-L (green) injections in the C2 whisker-responsive area, respectively, in PrV and SpVi nuclei of the trigeminal complex (left) or, respectively, in S1 and M1 cortices (middle). Injection sites are illustrated on Figure S1. Immunostaining for parvalbumin (blue) delineates VPM and thalamic reticular nucleus (RT). Red box (right) schematically highlights the thalamic areas seen on the left.

(F) Schematic view of the trigeminal and cortical projections to the thalamus is shown.

(G) Schematic map of the recorded labeled cells (filled symbols) and reconstructed tracks (open symbols) in the thalamus. Circles and diamonds refer to extracellular and intracellular recordings, respectively. This map results from the concatenation of seven successive coronal planes from 1.58 to 2.46 mm posterior relative to bregma.

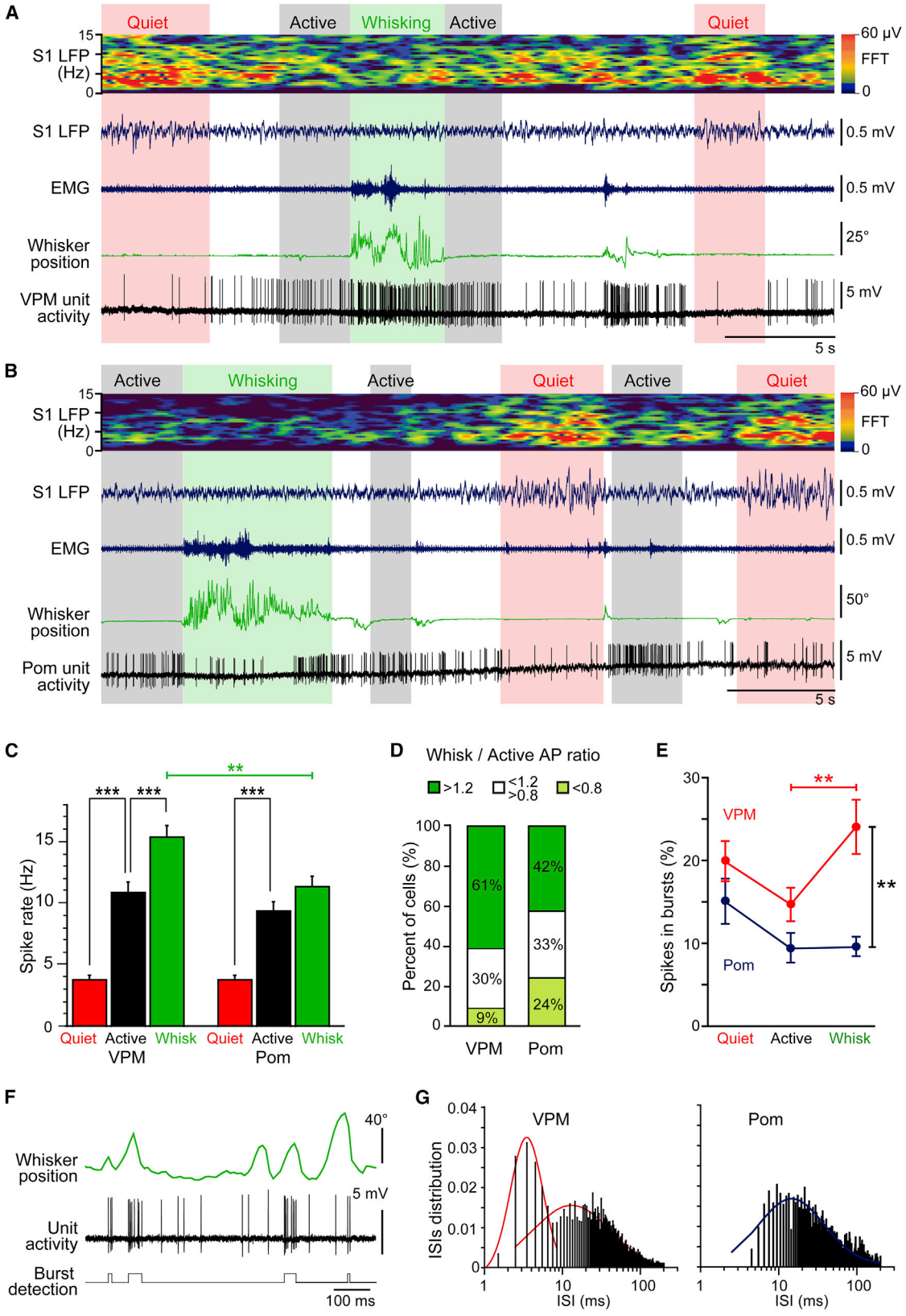

(legend on next page)

thalamic and cortical activity only during the quiet state (n = 52 and 29 cells, respectively).

Thalamic Membrane Potential Dynamics as a Function of Cortical State and Behavior

Intracellular recordings (Figures 3A–3C; Table S1) revealed that V_m in both VPM and Pom ($p < 0.05$ and $p < 0.01$, Friedman test) became more depolarized from quiet to whisking states (VPM: quiet −62.0 ± 1.8 mV, active −61.2 ± 2.3 mV, whisking −60.4 ± 2.1 mV, n = 8 cells; Pom: quiet −63.7 ± 2.1 mV, active −62.8 ± 2.2 mV, whisking −62.1 ± 2.1 mV, n = 6 cells). The V_m-SD increased significantly during whisking in VPM neurons ($p < 0.01$), but not Pom neurons. Remarkably, five of eight VPM cells did not fire any AP during quiet, active, and whisking states, while all Pom cells fired spikes in at least one of the three cortical states (Figure 3D). Intracellular recordings of spontaneously silent VPM neurons in awake mice are in agreement with previous data obtained under anesthesia (Brecht and Sakmann, 2002; Ganmor et al., 2010).

Interestingly, background synaptic activity was sufficiently low that we could identify putative individual excitatory postsynaptic potentials (EPSPs) in both cell types (Figures 3A and 3B). EPSPs were detected through an automatic template-matching procedure (see the Supplemental Experimental Procedures) and manually checked for consistency. EPSP rates increased significantly during whisking in VPM, but not in Pom, neurons compared to the active state (Figure 3E; VPM: quiet 9.7 ± 2.5 Hz, active 8.3 ± 2.4 Hz, whisking 12.8 ± 2.0 Hz, n = 8 cells; Pom: quiet 19.3 ± 3.7 Hz, active 22.0 ± 3.9 Hz, whisking 22.9 ± 4.2 Hz, n = 6 cells). Thus, the increased depolarization and V_m-SD observed in VPM during whisking could be due, in part, to an increase in synaptic activity (Figures 3A, 3E, and S3A).

Using a K-means clustering algorithm, we identified two populations of EPSPs in each thalamic nucleus on the basis of their rise time (Figure 3F; see the Supplemental Experimental Procedures). The rise time of fast-rising EPSPs was significantly shorter in VPM cells than in Pom neurons (fast-rising EPSPs, VPM: 0.24 ± 0.01 ms versus Pom: 0.36 ± 0.03 ms, $p < 0.05$ Mann-Whitney U test; slow-rising EPSPs, VPM: 0.60 ± 0.07 ms versus Pom: 0.63 ± 0.02 ms, $p = 0.36$), whereas peak amplitudes were not different between the two nuclei (fast-rising EPSPs, VPM: 3.7 ± 0.4 mV versus Pom: 2.6 ± 0.5 mV, $p = 0.09$; slow-rising EPSPs, VPM: 1.1 ± 0.2 mV versus Pom: 1.6 ± 0.3 mV, $p = 0.36$; Figures 3G and 3H). Fast-rising EPSPs were significantly more represented in all VPM cells than slow-rising EPSPs (86% ± 6% versus 14% ± 6% in whisking; Figure 3I), and their peak amplitudes were significantly larger than those of slow-rising EPSPs (Figures 3G and 3H). The ratio of fast and slow EPSPs did not change in VPM neurons comparing active and whisking periods, whereas for Pom neurons there was a significant increase in the fraction of slow-rising EPSPs during whisking (39% ± 15%) compared to active states (27% ± 9%; Figure 3I).

Whisker Position Encoding in VPM Cells

The V_m of cortical neurons exhibits whisking phase-locked fluctuations through sensory reafference (Poulet and Petersen, 2008), which are thus likely to be signaled via the thalamus. We therefore examined the spike timing of VPM and Pom cells relative to the whisking protraction-retraction cycles. Some VPM cells exhibited spiking at specific phases of the whisking cycle, which could occur during protraction (Figure 4A) or retraction (Figure 4B). For each VPM and Pom cell, we calculated the peristimulus time histogram (PSTH) of spikes aligned to peak whisker protraction and fitted a sinusoidal curve to compute phase preference and modulation strength (Figures 4A and 4B). The firing of VPM cells appeared to be more strongly modulated during the whisking cycle compared to Pom cells, without an obvious preferred phase (Figure 4C). Whereas 19% of VPM cells (8/41 cells) exhibited a whisking modulation index above 0.5, we did not find any Pom cells (0/24 cells) that were so strongly modulated (Figure 4D). The mean whisking modulation index across the population was significantly ($p < 0.001$) higher for VPM (0.32 ± 0.03, n = 41 cells) than Pom (0.19 ± 0.02, n = 24 cells) (Figure 4E).

It is noteworthy that the nine VPM cells with the highest fraction of spikes in bursts (>45%) all had above-average whisking-modulation indices (>0.3). In a statistical analysis of individual neurons, we found that the firing activity of 11 of 23 VPM cells was significantly modulated during whisking protraction-retraction cycles relative to shuffled data (Figures 4A and 4B; see the Supplemental Experimental Procedures). In contrast, only one of nine Pom neurons was significantly modulated (Figure S4A). Similarly, we calculated the PSTH of EPSPs aligned to peak whisker protraction for six VPM and six Pom cells recorded intracellularly (Figure S4B). The EPSP rates of two VPM cells showed significant phase-locked modulation with respect to the whisking protraction-retraction cycles. None of the Pom cells exhibited a significant whisking phase-locked EPSP rate modulation.

DISCUSSION

A number of studies in the literature, either in vitro or under anesthesia, describe the tight interplay between thalamic activity and cortical states (for reviews, see Steriade et al., 1993 and McCormick and Bal, 1997). Mechanistic understanding of what drives

Figure 2. Thalamic Firing as a Function of Cortical State and Behavior

(A and B) Two example thalamic cells recorded extracellularly, respectively, in VPM (A) and Pom (B) during quiet, active, and whisking states show (from top to bottom) the following: sliding window FFT (color graphs) of the S1-LFP (blue), neck EMG (blue), whisker position (green), and unit activity (black).

(C) Mean firing rate of thalamic cells recorded extracellularly (VPM, n = 56 cells; Pom, n = 33 cells). Data were compared across states using ANOVA for repeated measures or between VPM and Pom using unpaired t test.

(D) Distribution of the ratio of mean firing rates in whisking compared to active states is shown.

(E) Number of spikes in burst versus the total number of recorded spikes. Burst analysis was computed for cells displaying firing activity in all states (VPM, n = 49 cells; Pom, n = 29 cells). Ratios were compared across states using Friedman test or between VPM and Pom using Mann-Whitney test.

(F) Firing activity during whisking (green) for the cell shown in (A) at higher time resolution. The bottom trace indicates burst detection.

(G) Distribution of ISIs and log-normal curve fitting calculated during whisking for VPM (n = 28) and Pom (n = 9) cells. Only cells with more than 100 spikes were used for this analysis.

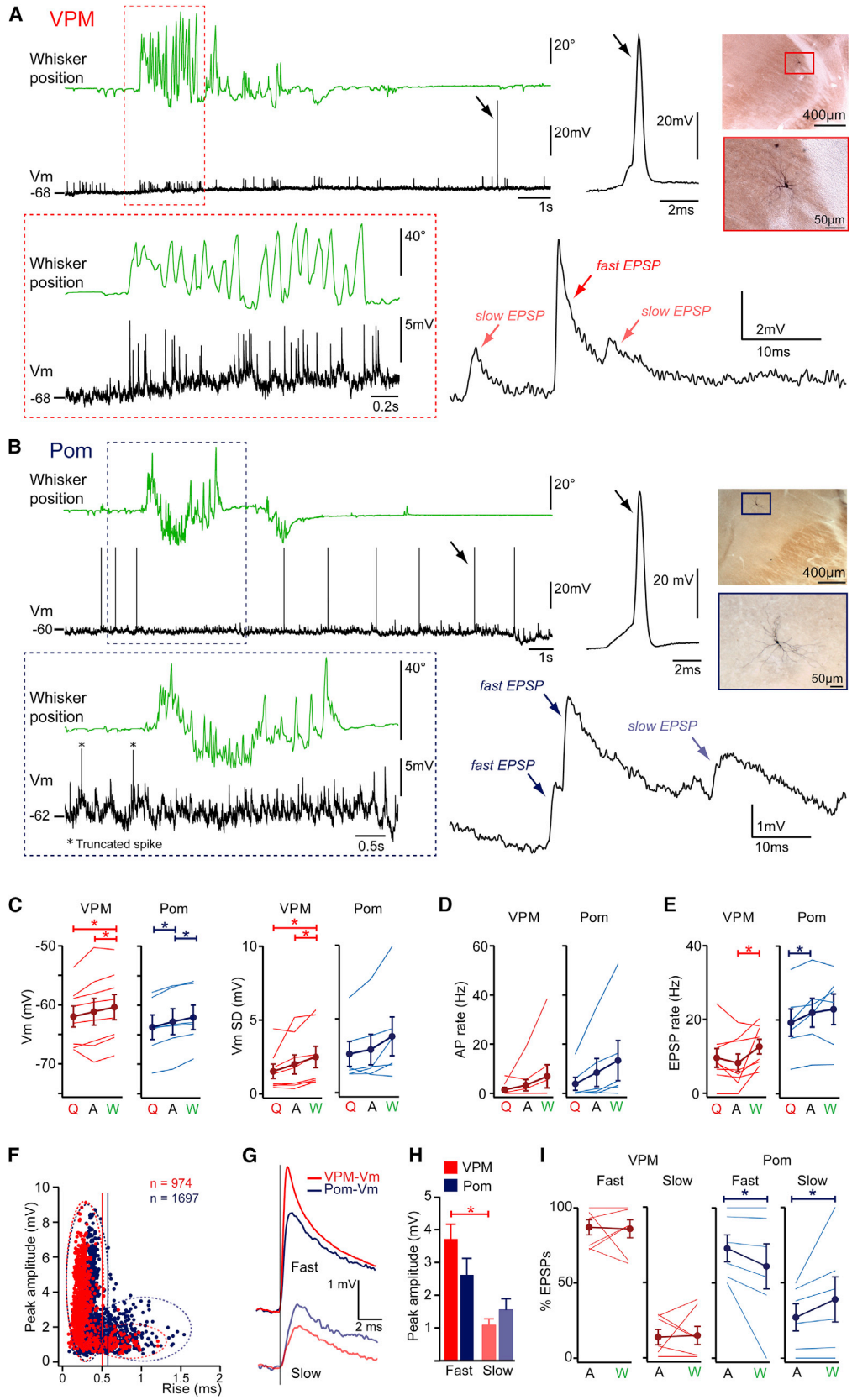

(legend on next page)

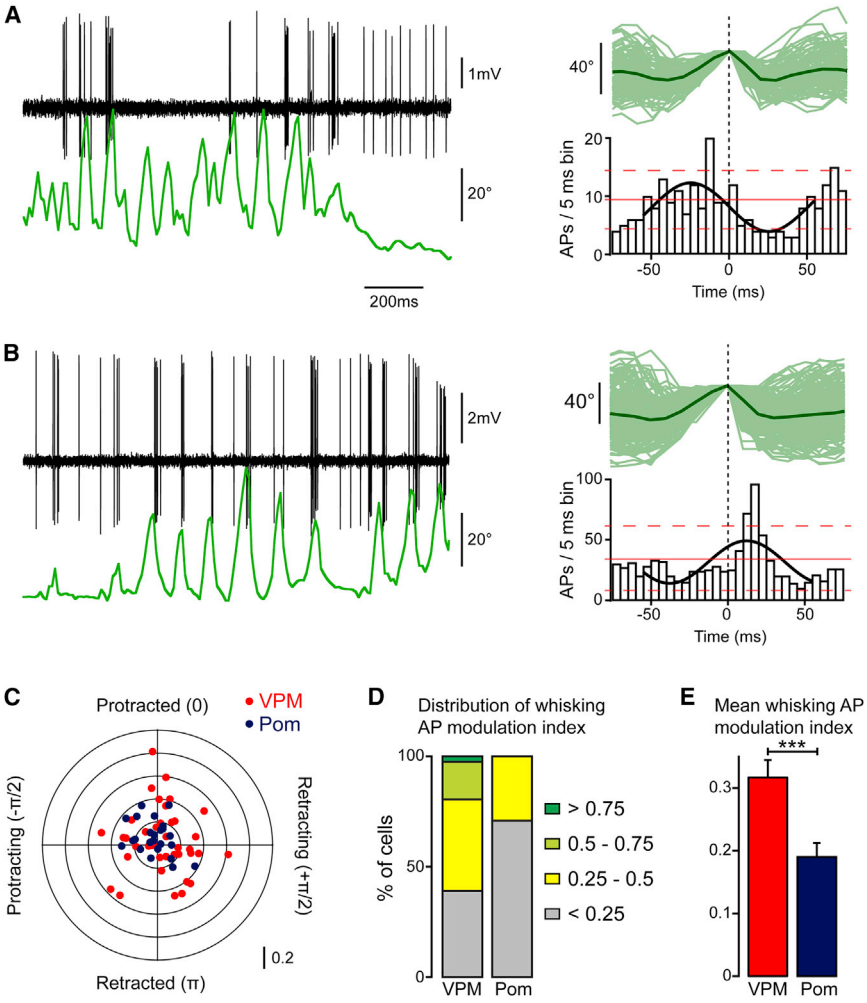

Figure 4. Thalamic Spike Timing on Whisking Cycles

(A and B) Example extracellular recordings of unit activity (black) in two VPM cells during whisking (green). These cells responded to deflection of the A2 whisker (A) or alpha whisker (B). Firing could correlate with the protraction (A) or the retraction (B) phase of the whisking cycle. Whisking cycles were collected (A, n = 113 whisking cycles; B, n = 244 whisking cycles), aligned at the peak of protraction and averaged (top green trace), and spikes occurring on whisking cycles were distributed in PSTHs (5-ms bins). Average (red line) and confidence intervals (one SD, dotted red lines) obtained by shuffling procedure of the spike times are represented (see Supplemental Experimental Procedures). The PSTH was fitted with a sinusoidal curve, giving a measure of the preferred phase and the amplitude of modulation of the cell firing during the whisking cycle.

(C) Fitting parameters plotted for all cells (VPM, n = 41; Pom, n = 24). Angle represents phase and radius shows the whisking modulation index (the fitted sinusoidal curve peak-trough amplitude in spike counts normalized by the mean spike count during whisking).

(D) Distribution of the whisking modulation index is shown.

(E) Average whisking modulation index in VPM and Pom (Mann-Whitney test) is shown.

AP firing requires intracellular recordings. However, to our knowledge, so far only a few intracellular studies have been performed in the thalamus of unanesthetized cats (Hirsch et al., 1983; Woody et al., 2003) and none in rodents, despite their increasing use as a model. In this paper, we show that thalamic firing and subthreshold activity are dynamically related to a variety of cortical and behavioral states in awake mice.

Our data show distinct whisker-related activity in VPM and Pom, with VPM neurons being more strongly modulated by whisking. However, we also found extensive heterogeneity within each thalamic nucleus, in agreement with previous studies reporting that these nuclei consist of an inhomogeneous set of specialized neurons

Figure 3. Thalamic V_m as a Function of Cortical State and Behavior

(A) V_m recorded in VPM during whisking transitions. V_m (black) was riddled with barrages of EPSPs during whisking (top and enlarged view in the red box). Arrows point out the enlarged view of an AP waveform (top right). Example trace shows individual fast- and slow-rising EPSPs (bottom right). The cell was labeled with Neurobiotin and recovered in VPM on coronal sections counterstained with cytochrome oxidase (right).

(B) V_m recorded in Pom during whisking transitions (top and enlarged view in the blue box). Arrows point out the enlarged view of an AP waveform (top right). Example trace shows individual fast- and slow-rising EPSPs (bottom right). The cell was labeled with Neurobiotin and recovered in Pom on coronal sections counterstained with cytochrome oxidase (right).

(C) Median and SD of V_m across quiet (Q), active (A), and whisking (W) states are shown.

(D) Mean firing rates of VPM and Pom cells recorded intracellularly. Five of eight VPM cells were silent during all waking states.

(E) Mean EPSP rates of VPM and Pom cells are shown.

(F) Individual EPSP peak amplitudes plotted against their rise time. Cluster analysis uncovered two populations of EPSPs in each nucleus, with a separation of 0.5 and 0.6 ms for VPM and Pom neurons, respectively (VPM, n = 974 EPSPs; Pom, n = 1,697 EPSPs).

(G) Grand average EPSP time course in VPM and Pom for fast-rising EPSPs (top) and slow-rising EPSPs (bottom) is shown.

(H) Average fast- and slow-rising EPSP peak amplitudes for VPM and Pom neurons are shown.

(I) Fraction of EPSPs classified as fast- and slow-rising in active (A) versus whisking (W) states per cell for VPM and Pom. Note the superposition of two VPM cells for 100% fast-rising EPSPs (and 0% slow-rising EPSPs).

In (C)–(I), the solid line represents the mean ± SEM; data were compared across states using Friedman and Wilcoxon tests or between nuclei using the Mann-Whitney test (mean ± SEM; VPM, n = 8 cells; Pom, n = 6 cells). In (G) and (I), n = 7 cells since one of eight VPM cells did not exhibit any EPSPs during quiet and active states (see E).

activated by specific conditions (Bruno et al., 2003; Timofeeva et al., 2003; Petersen et al., 2008). Part of this heterogeneity might result from differences in the anatomical locations of the cell bodies within Pom or within VPM barreloids. Diversity in thalamic responses during whisking also may reflect differences in motivation, whisking patterns, or other aspects of whisking behavior exhibited by awake rodents (Lenschow and Brecht, 2015).

We compared two distinct vigilance states without whisker movement, which we termed quiet and active. When mice entered a quiet state, slow oscillations appeared in S1-LFP, and both VPM and Pom thalamic cells displayed abrupt reductions in spontaneous firing rates (Figure 2) associated with V_m hyperpolarization (Figure 3). STAs of the S1-LFP revealed that AP firing in both VPM and Pom correlated with increased cortical activity during quiet states, but not during periods of desynchronized cortical activity (Figure S2). Thus, on average, VPM and Pom neurons showed a similar activity dependence when comparing quiet and active states in the absence of whisker movement.

In contrast, when mice were freely whisking in air, VPM and Pom cells on average showed distinct changes in activity. Averaged across the population, spike rates and bursting in VPM neurons, but not Pom neurons, increased during whisking compared to the active state (Figure 2). AP firing also was more strongly modulated by the phase of the whisking cycle in VPM neurons compared to Pom neurons (Figure 4). Mean EPSP rates also increased in VPM neurons during whisking, but not in Pom neurons (Figure 3). The synaptic input to VPM neurons was dominated by fast-rising EPSPs, which are thought to correspond to lemniscal driver synaptic inputs emanating from brainstem fibers (Castro-Alamancos, 2002; Deschênes et al., 2003; Ganmor et al., 2010), since in contrast with higher-order Pom cells, VPM cells only receive modulatory cortical inputs from layer 6 in S1 (Veinante et al., 2000; Killackey and Sherman, 2003). Our results, therefore, suggest that whisking increases firing in PrV, causing an increase in fast EPSPs in VPM neurons. The increased frequency of fast-rising EPSPs in VPM cells during whisking is likely to contribute to higher AP firing rates in VPM cells during whisking, as observed in the majority of VPM cells recorded extracellularly (Figure 2; Khatri et al., 2010).

The fast rise of these EPSPs combined with their large amplitude may drive precisely timed AP firing, able to precisely code whisker position/phase during the whisking cycle. Indeed, we identified a subset of VPM cells whose firing activity was driven by the whisking protraction-retraction cycles. Furthermore, our recordings in awake mice revealed an increase in bursts of APs associated with whisking specifically in VPM cells. Barrages of fast EPSPs appear to drive these bursts of APs, and we did not observe any low-threshold calcium spikes in our awake recordings. It is likely that T-type calcium channels are inactivated at the depolarized membrane potentials of VPM cells during whisking, and bursts driven by calcium spikes are thus unlikely (for review, see Llinás and Steriade, 2006). While the burst mode typically has been associated with anesthetized states and slow wave sleep, considerable evidence indicates that thalamocortical bursts also can occur in awake but inattentive quiet animals (Ramcharan et al., 2000; Swadlow and Gusev, 2001; Fanselow et al., 2001; Bezdudnaya et al., 2006). Bursts also were described during sensory processing, where they were shown to be reliably triggered by visual stimulation (Guido and Weyand, 1995; Wang et al., 2007). Burst firing has been suggested to play a specific role in information processing in the hippocampus (Lisman, 1997) and to facilitate transmitter release in the midbrain dopaminergic neurons (Gonon, 1988), as well as to be effective in activating cortical circuits (Swadlow and Gusev, 2001; Swadlow et al., 2002). Taken together, bursts would therefore allow rapid and efficient transmission of strong sensory events to be conveyed to the cortex. Burst firing in VPM neurons phase-locked to whisking might thus be an effective input to S1 cortex, enabling positional coding in V_m of neurons in S1 (Crochet and Petersen, 2006).

Although at a population level Pom cells did not increase AP firing rate during whisking compared to active states, we found that 42% of Pom cells increased firing by more than 20% and 24% of Pom cells decreased firing by more than 20% during whisking (Figure 2). What could be the underlying mechanisms for this observation? During whisking, Pom cells showed a decrease in fast-rising EPSPs, thought to arise from brainstem and S1-L5 driver inputs to Pom cells (Hoogland et al., 1991; Bourassa et al., 1995; Veinante et al., 2000; Lavallée et al., 2005; Groh et al., 2008, 2014). Thus, increased firing activity in some Pom cells during whisking does not appear to result from an increase in trigeminal inputs. In agreement with previous data (Aldes, 1988; Urbain and Deschênes, 2007a; Matyas et al., 2010), our tract-tracing experiments in mice indicated that cortical inputs from the motor cortex specifically innervate the Pom. Given its direct anatomical connections emanating from the motor cortex, the Pom indeed has been proposed to be involved in the pre-cortical encoding of whisker motion (Yu et al., 2006, 2015). Movement-related input to Pom also may be conveyed indirectly by modulation of the sensory cortex by motor cortex (Lee et al., 2008, 2013; Zagha et al., 2013) and/or by the VPM itself (thalamo-cortico-thalamic loop).

In Pom neurons, we described a significant increase in slow-rising EPSPs in whisking compared with active states, which could constitute putative corticothalamic synaptic events (Reichova and Sherman, 2004). The increase in the rate of slow-rising EPSPs during whisking in Pom (Figure 3) might, therefore, result from increased firing of corticothalamic neurons, which could increase firing rate in some Pom neurons during whisking. Our data do not rule out the possibility that trigeminal EPSPs in Pom may be shunted during whisking. It has been proposed that large multisynaptic GABAergic inputs arriving from extrareticular sources, the anterior pretectal nucleus (Bokor et al., 2005) and the zona incerta (Barthó et al., 2002), may have a major impact on Pom activity during whisking (Trageser and Keller, 2004; Lavallée et al., 2005; Urbain and Deschênes, 2007b). While we did not observe significant IPSPs in Pom neurons during whisking, our data do not rule out the possibility that shunting inhibition strongly contributes to the dampening of firing rates and excitatory synaptic activity in Pom cells (Lavallée et al., 2005). Indeed, we found about one-fourth of Pom cells decreased their firing specifically during whisking. In addition, the presence of multiple slow EPSPs during whisking might

contribute to increased membrane conductances of Pom cells and, by this means, participate in shunting excitatory driving inputs. Together with other recent studies (Groh et al., 2008, 2014; Slézia et al., 2011), our results suggest that Pom cells might be specialized for the processing of cortical feedback during active exploratory behavior; Pom may act as an integrator more than a detector of peripheral inputs.

Together, our data relate a heterogeneous and highly diverse awake state-dependent activity both in VPM and Pom. These results suggest a difference in coding whisker-related motion by VPM and Pom cells, and they shed light on the contribution of their respective excitatory inputs to the mechanisms underlying their firing activity.

EXPERIMENTAL PROCEDURES

Animals, Surgery, Training, and Data Collection

All experiments were carried out in accordance with the Swiss Federal Veterinary Office. Male 8- to 12-week-old C57BL6J mice were implanted under deep anesthesia with a lightweight metal head-holder and a recording chamber above the thalamus and S1. In addition, stainless steel screws and wires were inserted, respectively, over the skull and into neck muscles for the monitoring of EEG and EMG. After 2 days of recovery, repetitive daily training sessions of increasing duration were performed to habituate the mice to the head restraint. At the end of this training period, quiet wakefulness, slow wave sleep, and REM sleep episodes typically were observed, attesting that the restraint was well tolerated.

Small craniotomies were made under anesthesia over the C2 barrel column, functionally identified through intrinsic optical imaging, and over the thalamus. After 4–5 hr of recovery from anesthesia, electrophysiological recordings were performed while the whisker movements of the mouse were filmed simultaneously under infrared illumination using a high-speed camera (Figure 1A). Single units in the thalamus were recorded with glass micropipettes filled with a solution containing 1.5% Neurobiotin in 1 M potassium acetate (50–80 MOhms). Only high-quality sharp intracellular recordings with little (−0.3 nA, n = 2 cells) or no applied holding current (n = 12 cells) were taken into account. Cells exhibited >50 mV amplitude and <0.6 ms half-width spontaneous or evoked APs (<15% increase was tolerated in spike half-width during recordings). LFP recordings, in layer 4 or 5 of the S1-C2 column, were performed with glass micropipettes. Cell locations were determined by the intracellular or juxtacellular labeling of the last recorded unit (Pinault, 1996) and the reconstruction of each pipette track. At the end of the experiments, mice were perfused and brain sections processed for Neurobiotin histochemistry.

Data Analysis

Data analysis was performed with AxoGraph, Spike2, MiniAnalysis (Synaptosoft), MATLAB, IgorPro, OriginPro, and Excel software. Unless otherwise stated, results are reported as mean ± SEM. Statistics were performed using Statview and XLSTAT. The Bonferroni/Dunn correction was used when a post hoc test was applied. Significance levels were as follows: $^{*}p < 0.05$, $^{**}p < 0.01$, and $^{***}p < 0.001$.

SUPPLEMENTAL INFORMATION

Supplemental Information includes Supplemental Experimental Procedures, four figures, and one table and can be found with this article online at http://dx.doi.org/10.1016/j.celrep.2015.09.029.

AUTHOR CONTRIBUTIONS

N.U. and C.C.H.P. designed the project. N.U. performed the experiments. N.U., P.A.S., and L.J.G. analyzed the data. P.-A.L. wrote the whisker-tracking script. P.-A.L. and J.-C.C. wrote scripts for data analysis. N.U. and C.C.H.P. wrote the manuscript. P.A.S. and L.J.G. commented on the manuscript.

ACKNOWLEDGMENTS

We thank Ferenc Matyas and Monique Touret for fruitful discussions and critical help with anatomy. We thank the EPFL Faculty of Life Science Workshop and the ONCOFLAM laboratory, with Chantal Watrin, for help with instrumentation. We are grateful to Didier Pinault, Anita Lüthi, and Sylvain Crochet for critical reading of the manuscript. This work was funded by grants from the Swiss National Science Foundation (C.C.H.P.), the European Research Council (C.C.H.P.), and a Marie-Curie Re-integration Grant (N.U.).

Received: November 14, 2014
Revised: June 26, 2015
Accepted: September 9, 2015
Published: October 15, 2015

REFERENCES

Ahissar, E., Golomb, D., Haidarliu, S., Sosnik, R., and Yu, C. (2008). Latency coding in POm: importance of parametric regimes. J. Neurophysiol. *100*, 1152–1154, author reply 1155–1157.

Aldes, L.D. (1988). Thalamic connectivity of rat somatic motor cortex. Brain Res. Bull. *20*, 333–348.

Barthó, P., Freund, T.F., and Acsády, L. (2002). Selective GABAergic innervation of thalamic nuclei from zona incerta. Eur. J. Neurosci. *16*, 999–1014.

Bezdudnaya, T., Cano, M., Bereshpolova, Y., Stoelzel, C.R., Alonso, J.M., and Swadlow, H.A. (2006). Thalamic burst mode and inattention in the awake LGNd. Neuron *49*, 421–432.

Bokor, H., Frère, S.G., Eyre, M.D., Slézia, A., Ulbert, I., Lüthi, A., and Acsády, L. (2005). Selective GABAergic control of higher-order thalamic relays. Neuron *45*, 929–940.

Bosman, L.W.J., Houweling, A.R., Owens, C.B., Tanke, N., Shevchouk, O.T., Rahmati, N., Teunissen, W.H.T., Ju, C., Gong, W., Koekkoek, S.K.E., and De Zeeuw, C.I. (2011). Anatomical pathways involved in generating and sensing rhythmic whisker movements. Front. Integr. Neurosci. *5*, 53.

Bourassa, J., Pinault, D., and Deschênes, M. (1995). Corticothalamic projections from the cortical barrel field to the somatosensory thalamus in rats: a single-fibre study using biocytin as an anterograde tracer. Eur. J. Neurosci. *7*, 19–30.

Brecht, M., and Sakmann, B. (2002). Whisker maps of neuronal subclasses of the rat ventral posterior medial thalamus, identified by whole-cell voltage recording and morphological reconstruction. J. Physiol. *538*, 495–515.

Bruno, R.M., Khatri, V., Land, P.W., and Simons, D.J. (2003). Thalamocortical angular tuning domains within individual barrels of rat somatosensory cortex. J. Neurosci. *23*, 9565–9574.

Castro-Alamancos, M.A. (2002). Properties of primary sensory (lemniscal) synapses in the ventrobasal thalamus and the relay of high-frequency sensory inputs. J. Neurophysiol. *87*, 946–953.

Crochet, S., and Petersen, C.C.H. (2006). Correlating whisker behavior with membrane potential in barrel cortex of awake mice. Nat. Neurosci. *9*, 608–610.

Deschênes, M., Timofeeva, E., and Lavallée, P. (2003). The relay of high-frequency sensory signals in the Whisker-to-barreloid pathway. J. Neurosci. *23*, 6778–6787.

Deschênes, M., Timofeeva, E., Lavallée, P., and Dufresne, C. (2005). The vibrissal system as a model of thalamic operations. Prog. Brain Res. *149*, 31–40.

Fanselow, E.E., and Nicolelis, M.A.L. (1999). Behavioral modulation of tactile responses in the rat somatosensory system. J. Neurosci. *19*, 7603–7616.

Fanselow, E.E., Sameshima, K., Baccala, L.A., and Nicolelis, M.A. (2001). Thalamic bursting in rats during different awake behavioral states. Proc. Natl. Acad. Sci. USA *98*, 15330–15335.

Ganmor, E., Katz, Y., and Lampl, I. (2010). Intensity-dependent adaptation of cortical and thalamic neurons is controlled by brainstem circuits of the sensory pathway. Neuron *66*, 273–286.

Gonon, F.G. (1988). Nonlinear relationship between impulse flow and dopamine released by rat midbrain dopaminergic neurons as studied by in vivo electrochemistry. Neuroscience *24*, 19–28.

Groh, A., de Kock, C.P., Wimmer, V.C., Sakmann, B., and Kuner, T. (2008). Driver or coincidence detector: modal switch of a corticothalamic giant synapse controlled by spontaneous activity and short-term depression. J. Neurosci. *28*, 9652–9663.

Groh, A., Bokor, H., Mease, R.A., Plattner, V.M., Hangya, B., Stroh, A., Deschênes, M., and Acsády, L. (2014). Convergence of cortical and sensory driver inputs on single thalamocortical cells. Cereb. Cortex *24*, 3167–3179.

Guido, W., and Weyand, T. (1995). Burst responses in thalamic relay cells of the awake behaving cat. J. Neurophysiol. *74*, 1782–1786.

Hirsch, J.C., Fourment, A., and Marc, M.E. (1983). Sleep-related variations of membrane potential in the lateral geniculate body relay neurons of the cat. Brain Res. *259*, 308–312.

Hoogland, P.V., Wouterlood, F.G., Welker, E., and Van der Loos, H. (1991). Ultrastructure of giant and small thalamic terminals of cortical origin: a study of the projections from the barrel cortex in mice using Phaseolus vulgaris leuco-agglutinin (PHA-L). Exp. Brain Res. *87*, 159–172.

Khatri, V., Bermejo, R., Brumberg, J.C., and Zeigler, H.P. (2010). Whisking in air: encoding of kinematics by VPM neurons in awake rats. Somatosens. Mot. Res. *27*, 111–120.

Killackey, H.P., and Sherman, S.M. (2003). Corticothalamic projections from the rat primary somatosensory cortex. J. Neurosci. *23*, 7381–7384.

Kleinfeld, D., and Deschênes, M. (2011). Neuronal basis for object location in the vibrissa scanning sensorimotor system. Neuron *72*, 455–468.

Kleinfeld, D., Ahissar, E., and Diamond, M.E. (2006). Active sensation: insights from the rodent vibrissa sensorimotor system. Curr. Opin. Neurobiol. *16*, 435–444.

Lavallée, P., Urbain, N., Dufresne, C., Bokor, H., Acsády, L., and Deschênes, M. (2005). Feedforward inhibitory control of sensory information in higher-order thalamic nuclei. J. Neurosci. *25*, 7489–7498.

Lee, S., Carvell, G.E., and Simons, D.J. (2008). Motor modulation of afferent somatosensory circuits. Nat. Neurosci. *11*, 1430–1438.

Lee, S., Kruglikov, I., Huang, Z.J., Fishell, G., and Rudy, B. (2013). A disinhibitory circuit mediates motor integration in the somatosensory cortex. Nat. Neurosci. *16*, 1662–1670.

Lenschow, C., and Brecht, M. (2015). Barrel cortex membrane potential dynamics in social touch. Neuron *85*, 718–725.

Lisman, J.E. (1997). Bursts as a unit of neural information: making unreliable synapses reliable. Trends Neurosci. *20*, 38–43.

Llinás, R.R., and Steriade, M. (2006). Bursting of thalamic neurons and states of vigilance. J. Neurophysiol. *95*, 3297–3308.

Masri, R., Bezdudnaya, T., Trageser, J.C., and Keller, A. (2008). Encoding of stimulus frequency and sensor motion in the posterior medial thalamic nucleus. J. Neurophysiol. *100*, 681–689.

Matyas, F., Sreenivasan, V., Marbach, F., Wacongne, C., Barsy, B., Matéo, C., Aronoff, R., and Petersen, C.C.H. (2010). Motor control by sensory cortex. Science *330*, 1240–1243.

McCormick, D.A., and Bal, T. (1997). Sleep and arousal: thalamocortical mechanisms. Annu. Rev. Neurosci. *20*, 185–215.

Petersen, R.S., Brambilla, M., Bale, M.R., Alenda, A., Panzeri, S., Montemurro, M.A., and Maravall, M. (2008). Diverse and temporally precise kinetic feature selectivity in the VPm thalamic nucleus. Neuron *60*, 890–903.

Pinault, D. (1996). A novel single-cell staining procedure performed in vivo under electrophysiological control: morpho-functional features of juxtacellularly labeled thalamic cells and other central neurons with biocytin or Neurobiotin. J. Neurosci. Methods *65*, 113–136.

Poulet, J.F.A., and Petersen, C.C.H. (2008). Internal brain state regulates membrane potential synchrony in barrel cortex of behaving mice. Nature *454*, 881–885.

Poulet, J.F.A., Fernandez, L.M., Crochet, S., and Petersen, C.C.H. (2012). Thalamic control of cortical states. Nat. Neurosci. *15*, 370–372.

Ramcharan, E.J., Gnadt, J.W., and Sherman, S.M. (2000). Burst and tonic firing in thalamic cells of unanesthetized, behaving monkeys. Vis. Neurosci. *17*, 55–62.

Reichova, I., and Sherman, S.M. (2004). Somatosensory corticothalamic projections: distinguishing drivers from modulators. J. Neurophysiol. *92*, 2185–2197.

Slézia, A., Hangya, B., Ulbert, I., and Acsády, L. (2011). Phase advancement and nucleus-specific timing of thalamocortical activity during slow cortical oscillation. J. Neurosci. *31*, 607–617.

Steriade, M., McCormick, D.A., and Sejnowski, T.J. (1993). Thalamocortical oscillations in the sleeping and aroused brain. Science *262*, 679–685.

Swadlow, H.A., and Gusev, A.G. (2001). The impact of 'bursting' thalamic impulses at a neocortical synapse. Nat. Neurosci. *4*, 402–408.

Swadlow, H.A., Gusev, A.G., and Bezdudnaya, T. (2002). Activation of a cortical column by a thalamocortical impulse. J. Neurosci. *22*, 7766–7773.

Timofeeva, E., Mérette, C., Emond, C., Lavallée, P., and Deschênes, M. (2003). A map of angular tuning preference in thalamic barreloids. J. Neurosci. *23*, 10717–10723.

Trageser, J.C., and Keller, A. (2004). Reducing the uncertainty: gating of peripheral inputs by zona incerta. J. Neurosci. *24*, 8911–8915.

Urbain, N., and Deschênes, M. (2007a). A new thalamic pathway of vibrissal information modulated by the motor cortex. J. Neurosci. *27*, 12407–12412.

Urbain, N., and Deschênes, M. (2007b). Motor cortex gates vibrissal responses in a thalamocortical projection pathway. Neuron *56*, 714–725.

Veinante, P., Jacquin, M.F., and Deschênes, M. (2000). Thalamic projections from the whisker-sensitive regions of the spinal trigeminal complex in the rat. J. Comp. Neurol. *420*, 233–243.

Wang, X., Wei, Y., Vaingankar, V., Wang, Q., Koepsell, K., Sommer, F.T., and Hirsch, J.A. (2007). Feedforward excitation and inhibition evoke dual modes of firing in the cat's visual thalamus during naturalistic viewing. Neuron *55*, 465–478.

Woody, C.D., Gruen, E., and Wang, X.F. (2003). Electrical properties affecting discharge of units of the mid and posterolateral thalamus of conscious cats. Neuroscience *122*, 531–539.

Yu, C., Derdikman, D., Haidarliu, S., and Ahissar, E. (2006). Parallel thalamic pathways for whisking and touch signals in the rat. PLoS Biol. *4*, e124.

Yu, C., Horev, G., Rubin, N., Derdikman, D., Haidarliu, S., and Ahissar, E. (2015). Coding of object location in the vibrissal thalamocortical system. Cereb. Cortex *25*, 563–577.

Zagha, E., and McCormick, D.A. (2014). Neural control of brain state. Curr. Opin. Neurobiol. *29*, 178–186.

Zagha, E., Casale, A.E., Sachdev, R.N., McGinley, M.J., and McCormick, D.A. (2013). Motor cortex feedback influences sensory processing by modulating network state. Neuron *79*, 567–578.